PCCP

PAPER

Cite this: *Phys. Chem. Chem. Phys.*, 2017, **19**, 3894

Gas diffusion on graphene surfaces

Chengzhen Sun and Bofeng Bai*

Received 11th September 2016,
Accepted 7th December 2016

DOI: 10.1039/c6cp06267a

www.rsc.org/pccp

Graphene provides a possibility where gas adsorption energy is comparable with molecular collision energy for physically adsorbed gases, resulting in the incompetence of the traditional hopping model to describe graphene-related surface diffusion phenomena. By calculating surface diffusion coefficients based on the Einstein equation, we exactly demonstrate that the gas diffusion on a graphene surface is a two-dimensional gas behavior mainly controlled by the collisions between adsorbed molecules. The surface diffusion on the graphene film just follows the bulk diffusion qualitatively, namely the diffusion coefficients decrease with increasing gas pressure. Quantitatively, the surface diffusion coefficients are lower than the bulk diffusion coefficients, predicted using the hard sphere model, owing to the restriction of graphene films. The reduction in diffusion coefficient is related to the simultaneously suppressed average frequency of molecular collisions and the average travelling distance between successive collisions. In addition, a lower diffusion coefficient on a hydrogen-functionalized graphene surface is identified, caused by the blocking effects of chemical functional groups.

Introduction

The diffusion of gas molecules on solid surfaces is a very common phenomenon, but it has remained a subject of unfailing charm for the research communities.[1–4] Surface diffusion is distinguished from bulk diffusion by whether the gas molecules adsorbed onto solid surfaces or not. In the adsorption layer on a solid surface, gas diffusion in the direction perpendicular to the solid surface is restricted. Surface diffusion is determined not only by the interactions among gas molecules but also by the interactions between gas molecules and solid materials. Therefore, surface diffusion is affected by the gas species, the solid properties and their surface structure, and the pressure-dependent gas coverage of the surface. It is generally accepted that surface diffusion is driven by the chemical potential gradient on the solid surface and the diffusion barrier is related to the adsorption energy of gas molecules. Accordingly, the hopping (jumping) model[5–8] is widely applied to describe the surface diffusion phenomenon as a process where the adsorbed molecules hop between adjacent adsorption sites on the solid surface. For most of the gas–solid systems that display gas adsorption energy far exceeding the thermal energy of translation (gas collision energy), the surface diffusivity increases with the increase of pressure, because the gas adsorption energy decreases with increasing molecular concentration and the progressive filling of adsorption sites of weakening energy enhances the molecular mobility. The opposite trend between surface diffusivity and pressure is possible if the thermal energy of translation is comparable with the adsorption energy. In this case, the two-dimensional gas behavior occurs, which is controlled by collisions between adsorbed molecules and characterized by a surface mean free path. The surface mean free path greatly exceeds the spacing distance between adjacent adsorption sites, such that the hopping mechanism cannot be competent. Although the researchers[5,7] have speculated that the hopping model may not be competent in the case of extremely weak adsorption, the surface diffusion phenomenon under the condition that gas adsorption energy is comparable with gas collision energy has not been examined by other researchers systematically, because it is very difficult to find such solid materials to meet this conditions even in the premise of physical adsorption.

Graphene,[9,10] a two-dimensional atomic thickness material, has a broad application prospect in many gas-related industries. In the gas separation industries,[11–13] the graphene with nanopores is a very promising separation membrane based on the molecular size-sieving effects. The molecular permeation through graphene nanopores is greatly affected by the gas adsorption on the graphene surface,[14–16] which exerts a positive surface flux described by Fick's law (as shown in our early work[17]); the surface flux is determined by the surface diffusion coefficient and the molecular density gradient on the graphene surface. Namely, the surface diffusion of gas molecules on graphene greatly affects the molecular permeation abilities through graphene nanopores and finally the permeability of these novel graphene-based gas separation membranes. Meanwhile, the gas intercalation underneath graphene is also related to the surface diffusion ability.[18–20]

State Key Laboratory of Multiphase Flow in Power Engineering, Xi'an Jiaotong University, Shaanxi 710049, China. E-mail: bfbai@mail.xjtu.edu.cn

For hydrogen storage,[21–24] graphene has also shown a great promise owing to their strong affinity to hydrogen, low gravimetric density and conveniences in the realization of hydro/dehydrogenation processes. Therefore, the hydrogen adsorption and diffusion characteristics on the graphene surface definitely affect the hydrogen storage ability and efficiency. In the graphene-based gas sensors,[25,26] the gas adsorption and diffusion on the graphene surface basically determine the sensitivity of the sensors by affecting the electron transport through graphene. In short, the gas diffusion on the graphene surface is very crucial for many gas-related applications of graphene materials.

Compared to the surface diffusion on other solid materials, the gas diffusion on the graphene surface exhibits several distinctive characteristics, as follows. (1) Graphene is a one-atomic layer film consisting of carbon atoms and thus the physical interactions between gas molecules and graphene are not very strong and even comparable with the interactions among gas molecules. Therefore, graphene provides a possibility where the gas collision energy is comparable with the gas adsorption energy for the physically adsorbed gases. (2) Only a monolayer of gas molecules can adsorb on the graphene surface, thus the molecular exchanges among adsorbed layers are not considered in the analysis of surface diffusion; however, a frequent molecular exchange appears between the adsorption layer and the bulk phase by means of molecular adsorption and desorption. (3) Graphene is a two-dimensional sheet with honeycomb crystal lattices essentially consisting of sp^2-bonded carbon atoms. This special surface crystal structure may induce some distinct gas diffusion phenomena on the graphene surface. Since the birth of graphene, to the best of our knowledge, there has been no literature study of the gas diffusion characteristics on graphene surfaces, although the diffusion of adsorbed atoms and ions on the graphene surface were studied appropriately.[27–31] Therefore, a comprehensive investigation on the surface diffusion coupling with a graphene material is urgently needed.

To better understand the surface diffusion phenomenon, the investigations on how the gas molecules move on the solid surface are of crucial importance. The gas diffusion on the graphene surface occurs in the adsorption layer of sub-nanometers, thus the surface diffusion phenomenon must be investigated at the molecular levels. The molecular dynamics (MD) method is a computational simulation tool capturing the movements of atomic particles controlled by Newton's laws of motion and therefore it can investigate the nanoscale transport phenomena accurately at the molecular levels.[32–35] Therefore, we present a systematical study of the gas diffusion on the graphene surface from molecular insights using the MD simulation method. The surface diffusion coefficient is obtained statistically based on the Einstein equation and analyzed from the aspects of molecular isothermal adsorption characteristics, molecular kinetic motion on the graphene surface, *etc.* We show that the gas diffusion on the graphene surface is a two-dimensional gas behavior mainly controlled not by the hopping mechanism but by the molecular collisions, and the surface diffusion coefficients decrease with the increase of pressure. However, the surface diffusion coefficients present a large discrepancy with the theoretical values of bulk diffusion coefficients predicted from the ideal gas kinetic theory. In addition, it is found that the hydrogen functionalization of the graphene surface can reduce the diffusion coefficient considerably.

Simulation model

We present the MD simulations in a straightforward system, where the gas molecules are placed on the top of a square single-layer graphene (3 nm × 3 nm), as shown in Fig. 1(a). The molecules are confined in a simulation box through periodic boundary conditions in the directions parallel to the graphene surface and reflective boundary conditions in the direction vertical to the graphene surface. In the simulations, we place 50 gas molecules on the top of graphene, but the height of simulation box varies so that different gas pressures are involved. In this case, a simulation box with more molecules only brings a larger gas phase zone and cannot affect the molecular diffusions on the graphene surface, because most of the computational cost is spent on simulating the molecular motions in the gas phase far away the graphene surface. We consider the initial pressure of the uniformly distributed molecules as a variable parameter from 10 bar to 55 bar; correspondingly, the height of the simulation box varies from 22.5 nm to 4.3 nm. The CH_4 and CO_2 molecules are investigated in this study, because they can strongly adsorb on the graphene surface and exhibit an obvious surface diffusion phenomenon; the configurations of these two molecules are shown in Fig. 1(b and c). In order to better analyze the surface diffusion characteristics, the graphene atoms are fixed in the simulations to neglect the weak vibrations of the graphene film resulting from the collisions with gas molecules. A simulation case is firstly run for 50 million timesteps to reach a complete equilibrium state. Then, 2 million timesteps are run to record the movement of gas molecules on the graphene surface with a recording period of only 250 timesteps; this simulation period is determined to ensure a large sample set where hundreds of molecular samples diffusing on the graphene surface, because one molecule can repeatedly enter the surface zone and return to the gas phase many times. As the

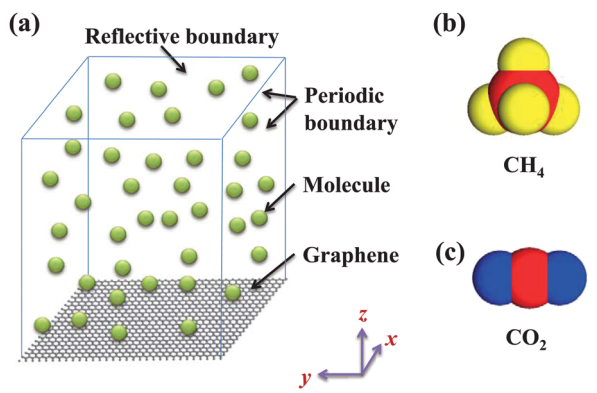

Fig. 1 Simulation model of gas diffusion on graphene surface. (a) A cubic simulation box. (b and c) Atomic model of CH_4 and CO_2 molecules, respectively.

simulation periods for calculating diffusion coefficients increase from 1 million to 5 million timesteps, the calculated diffusion coefficients present a relative standard deviation of only 2.63%. Therefore, the 2 million time step run is adequate to obtain a relatively large sample set and accordingly a high accuracy in the calculation of diffusion coefficient. In the simulations the time step is set to be 0.134 fs, such that the average molecular moving length in the recording period (33.5 fs) is in the order of 10^{-2} nm and thus the movement trajectories of gas molecules on the graphene surface can be repeated with a high resolution. The system temperature is kept at 300 K in a *NVT* ensemble. The small time step applied in the simulations can also produce a weak fluctuation of the system temperature.

To model the interactions among gas molecules and graphene, several different potential models are applied. For the graphene carbon atoms, the simple Lennard-Jones (L-J) potential model is employed. For CH_4 molecules, the AIREBO potential model is applied, which is very suitable for modeling the atomic interactions in hydrocarbons; the form and corresponding parameters of the AIREBO model can be found in the work by Stuart *et al.*[36] Many MD simulation works for hydrocarbons,[37–40] including our previous works,[14,15,17] were performed based on the AIREBO potential. The comparative simulations with the AIREBO model and the traditional L-J model show small deviations between the simulation results of the molecular sample number on the graphene surface and surface diffusion coefficients for CH_4 molecules (the average relative deviations are 4.98% and 4.18%, respectively). For the polar CO_2 molecules, the L-J potential model coupling with a Coulombic term is applied, as follows:

$$\phi(r_{ij}) = \begin{cases} 4\varepsilon\left[\left(\frac{\sigma}{r_{ij}}\right)^{12} - \left(\frac{\sigma}{r_{ij}}\right)^{6}\right] + \frac{Cq_iq_j}{\chi r_{ij}} & (r_{ij} < r_{\text{cut}}) \\ 0 & (r_{ij} \geq r_{\text{cut}}) \end{cases} \quad (1)$$

where σ and ε are the length and energy parameter in the L-J potential term, respectively; in the Coulombic term, q_i and q_j are the atomic charges, χ is the dielectric constant, and C is the energy-conversion constant. The interactions between carbon atoms in graphene and atoms in gas molecules are also modeled using the hybrid potential model; the L-J potential parameters between crossing atoms are evaluated using the Lorentz–Berthelot mixing rule. The parameters involved in the hybrid potential model are listed in Table 1. It is noted that the bond information, including bond stretch and angle deformation, in CH_4 and CO_2 gas molecules are considered in our simulations; the bond information in CH_4 molecules is included in the AIREBO model, and that in CO_2 molecules is considered by the harmonic model (see the work by Harris *et al.*[41])

Table 1 Parameters in the hybrid potential model involved in the simulations

	ε (ev)	σ (Å)	Charge (e)
C_1–C_1[42 a]	2.413×10^{-3}	3.400	—
C_3–C_3[43]	2.424×10^{-3}	2.757	0.6512
C_3–O	4.101×10^{-3}	2.895	—
O–O[43]	6.938×10^{-3}	3.033	−0.3256
C_1–C_2[42]	2.413×10^{-3}	3.400	—
C_1–H[44]	1.771×10^{-3}	2.950	—
C_1–C_3	2.418×10^{-3}	3.079	—
C_1–O	4.092×10^{-3}	3.217	—

[a] 1 represents graphene carbon atoms, 2 represents carbon atoms in CH_4 molecules, and 3 represents carbon atoms in CO_2 molecules.

Results and discussion

Gas adsorption

Due to the interactions between gas molecules and graphene atoms, the gas molecules can adsorb onto the graphene surface to form a high-density zone (denoted as adsorption layer). The surface diffusion phenomenon just occurs in the adsorption layer. Therefore, it is very crucial to investigate the gas adsorption characteristics on the graphene surface to deeply understand the surface diffusion phenomenon. Fig. 2 shows the molecular density distribution along the direction perpendicular to the graphene surface for CH_4 and CO_2 molecules at different pressures. As firstly seen from the figure, the molecular density distribution is not uniform and a high-density

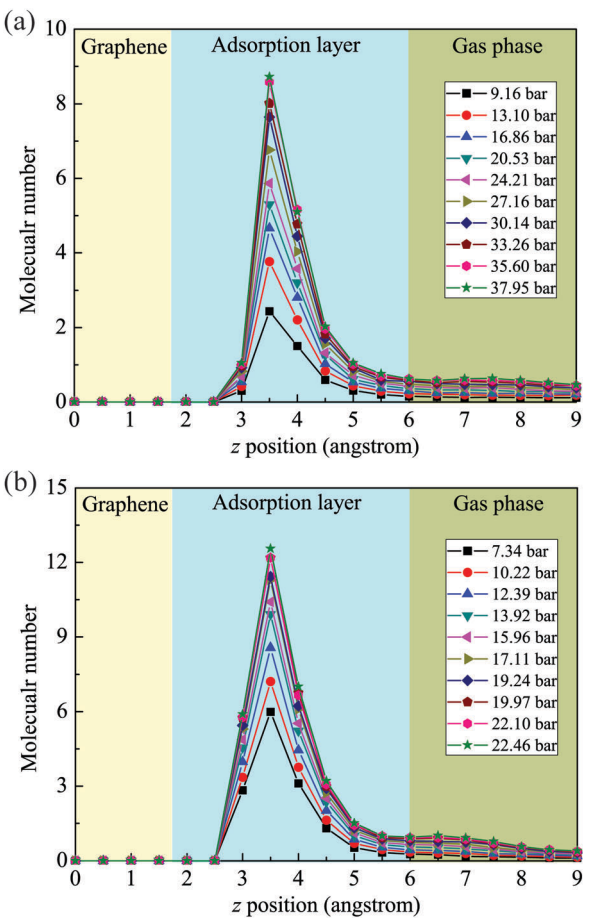

Fig. 2 Molecular number density distribution along the direction perpendicular to graphene surface for (a) CH_4 and (b) CO_2, respectively. Graphene zone, adsorption layer and gas phase are distinguished.

zone appears on the graphene surface, meaning that the gas molecules indeed adsorb on the graphene surface. Away from the high-density zone, the molecular density distributes uniformly and the molecules in this zone behave as a normal gas phase. The adsorption layer is demarcated with the gas phase at z_m = 0.6 nm according to the molecular density distribution. Thus, the surface diffusion is restricted in the zone 0.17 nm < z_m < 0.6 nm, where the value 0.17 nm is determined by the thickness of graphene. Importantly, the monolayer adsorption characteristics on the graphene surface can be concluded from the equivalence between the adsorption layer thickness and the molecular diameter.

We also see from Fig. 2 that the gas adsorption intensities are directly proportional to the gas pressure; the higher the gas pressure, the stronger the gas adsorption intensity. At the same pressure, the adsorption intensity of CO_2 molecules is higher than that of CH_4 molecules for the stronger interactions between CO_2 molecules and graphene atoms. It is noted that the pressure values shown in this figure are the pressures of the gas phase, which are calculated from the average molecular number in the gas phase and the volume of the gas phase zone based on the ideal gas state equation. In order to further study the effects of gas pressure on gas adsorption intensity, we obtain the isothermal adsorption characteristics of gas molecules on the graphene surface, as shown in Fig. 3. It is found that the adsorbed molecular number increases sharply with increasing pressure at lower pressures and it increases slowly at higher pressures. Recalling the monolayer adsorption characteristics of gas molecules on the graphene surface, it is suggested that the gas molecular adsorption characteristics on the graphene surface can be reasonably described using the Langmuir adsorption isotherm,

$$N_a = N_{a,m}\frac{kP}{1+kP} \quad (2)$$

where P is the gas pressure, k is the Langmuir adsorption constant, N_a is the number of adsorbed molecules on the graphene surface and $N_{a,m}$ is the maximum value of N_a. The fitted curves of the Langmuir adsorption isotherm are also shown in Fig. 3.

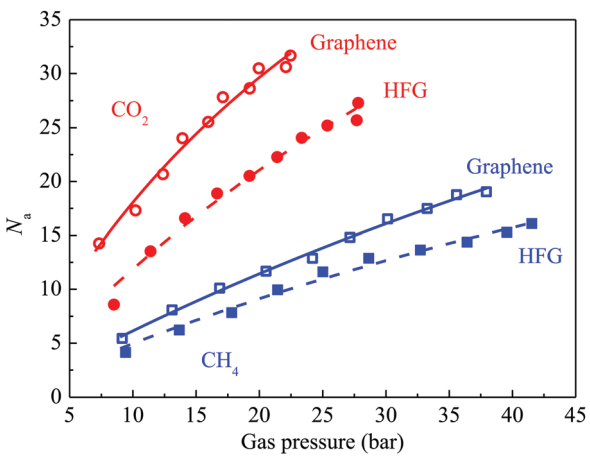

Fig. 3 Langmuir isothermal adsorption characteristics of gas molecules on graphene surface.

Diffusion coefficient

Then, we obtain the diffusion coefficient D based on the Einstein equation, in which the diffusion coefficient is calculated from the slope of the linear relationship between mean-square-displacement and time. The form of the Einstein equation is as follows:

$$D = \frac{\langle (x-x_0)^2 + (y-y_0)^2 \rangle}{4\Delta t_r} \quad (3)$$

where x_0 and y_0 are the x- and y-coordinates at t = 0, x and y are the coordinates after a residence time of Δt_r in the adsorption layer. It is noted that t = 0 represents the time that a molecule just enters into the adsorption layer. The schematic model for calculating diffusion coefficient on the graphene surface is given in Fig. 4(a). In the entire simulation period, a molecule can enter into and move out the adsorption layer repeatedly; therefore, the sample set of gas molecules moving on the graphene surface is very huge. For different samples of molecules moving on the graphene surface, the residence time in the adsorption layer is different. Fig. 4(b and c) show the total number of samples *versus* the time that a molecule can at least stay in the adsorption layer during the simulation period of 2 million timesteps. The curves descend sharply at the beginning, indicating that a majority of molecules stay in the adsorption layer only for a very short time period. The total sample number corresponding to the left end point of the curve is related to the molecular kinetic motion; a higher number means more molecules entering into the adsorption layer. The time corresponding to the right end point of the curve is the longest residence time for all the samples.

As seen from the curves and inserted maps in Fig. 4(b and c), the total number of molecules that enter into the adsorption layer increases with increasing pressure. This number can be basically predicted using the ideal gas kinetic theory. In an ideal gas, the flux of point particles through a surface plane (J, in the unit of mol m^{-2} s^{-1}) is calculated exactly by:

$$J = \frac{P}{\sqrt{2\pi RMT}} \quad (4)$$

where P is gas pressure, R is the universal gas constant, M is molar mass, and T is temperature. Therefore, the number of molecules (N_I) that can enter into the adsorption layer in a simulation time interval of Δt_s is

$$N_I = N_A A_s \Delta t_s \frac{P}{\sqrt{2\pi RMT}} \quad (5)$$

where N_A is the Avogadro constant and A_s is the area of the graphene surface. It can be found from the inserted maps that the ideal gas kinetic theory basically underestimates the values of N_I, especially for the CO_2 molecules, because many molecules can stay in the adsorption layer for a very short time period, meaning that these molecules do not adsorb on the graphene surface effectively. Thus, the number N_I obtained in the

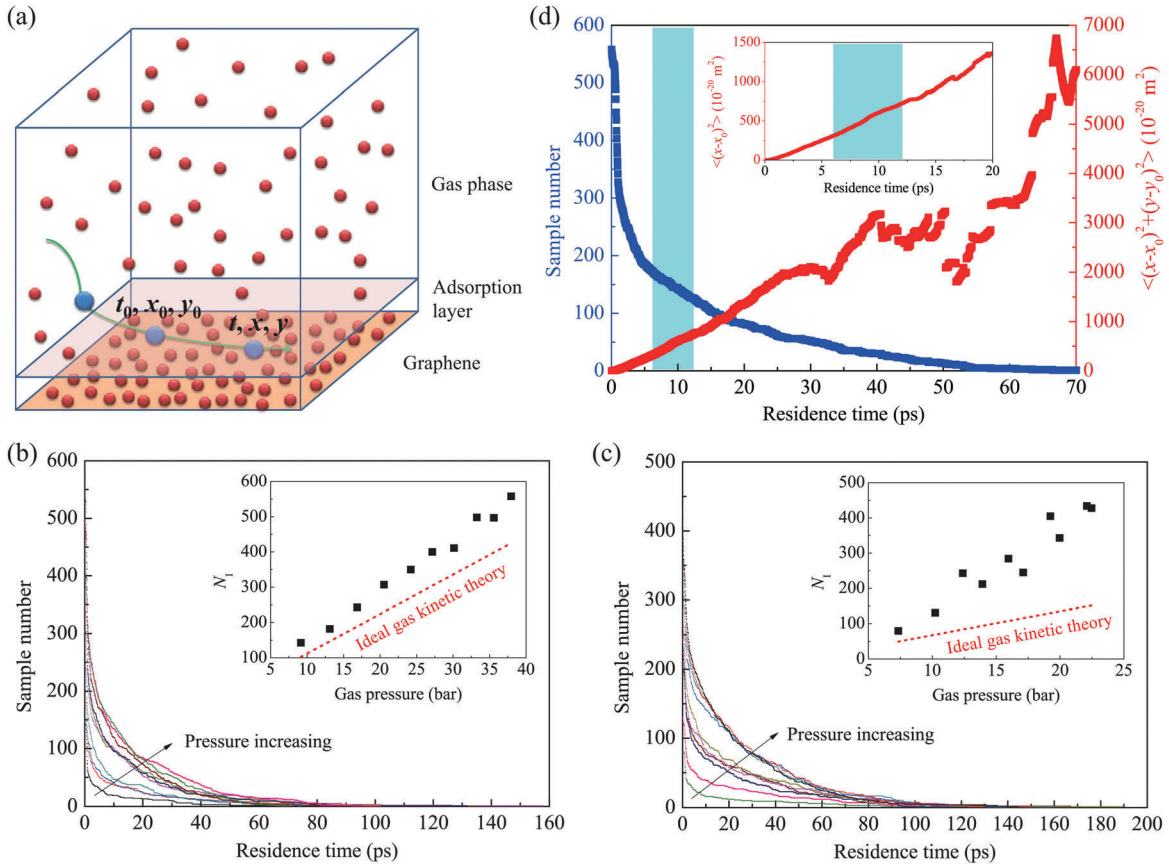

Fig. 4 Calculation method of diffusion coefficient on graphene surface. (a) Model for the calculation of diffusion coefficient using the Einstein equation. (b and c) Sample number *versus* the corresponding residence time in adsorption layer for CH_4 and CO_2 molecules, respectively. Inseted figures show the total number of molecules entering into the adsorption layer at different pressures. (d) Fitting of the diffusion coefficient based on the correlation between mean-square-displacement in the x–y plane and residence time. Inseted figure gives an enlargement of the light green zone.

simulations involves the number of invalidly adsorbed molecules, resulting in the underestimation of the ideal gas kinetic theory. We note that the deviations between theoretical values and simulation values of N_I are larger at higher pressures, because at higher pressures the molecules distribute densely on the graphene surface and the partly-adsorbed molecules can be easily pushed out.

A curve of the sample number *versus* the residence time corresponds to a straight line of mean-square-displacement in the x–y plane *versus* time, as seen from Fig. 4(d), which gives an example for CH_4 molecules at an initial pressure of 55 bar. For the left-part of the curve (line), the partly-adsorbed molecules move out of the adsorption layer promptly and they do not effectively diffuse on the graphene surface. For the right-part of the curve (line), the adsorbed molecules have diffused on the graphene surface for a relatively long time period, but the total number of such samples is not adequate to obtain an effective mean-square-displacement (*e.g.* there are only 52 molecular samples which can stay at least 30 ps on the graphene surface); in this part, the line of mean-square-displacement *versus* time is discontinuous due to the limited sample number. Therefore, only the central-part of the line (highlighted by light green in Fig. 4(d)) can be employed to calculate the diffusion coefficient based on the Einstein equation. In the calculation of diffusion coefficient, the left boundary of the central-part is related to the decline pattern of the curve while the right boundary of the central-part is decided by the appearance of the discontinuous line. The determination of the central-part can bring an uncertainty in the calculation of diffusion coefficients; however, this part of uncertainty is hard to be quantified. Therefore, we carefully determine the central-part with a good linearity to ensure a small uncertainty.

Based on the method described above, we can calculate the diffusion coefficients of CH_4 and CO_2 molecules on the graphene surface at different pressures. As seen from Fig. 5, the diffusion coefficient decreases with increasing gas pressure. Owing to the one-atomic thickness of graphene, the gas adsorption energy on the graphene surface is weak and even comparable with the collision energy among gas molecules, accordingly the surface diffusion process is mainly controlled by the collisions between adsorbed molecules. At higher pressures, the free motions of gas molecules are weakened for the higher molecular density, inducing a decrease in the diffusion coefficient with the increase of gas pressure. Therefore, the gas diffusion on the graphene surface approaches bulk phase gas behavior and exhibits two-dimensional characteristics. Consequently, the

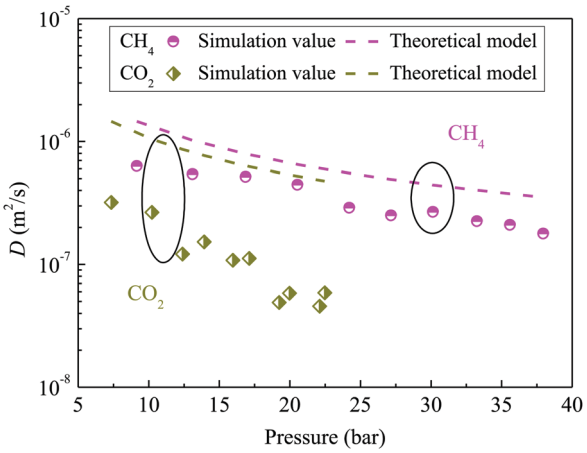

Fig. 5 Surface diffusion coefficients of CH_4 and CO_2 molecules at different pressures. The dash lines denote the theoretical values of bulk diffusion coefficients predicted using the hard sphere model based on the ideal gas kinetic theory.

traditional hopping model for surface diffusion definitely fails to describe the gas diffusion phenomenon on the graphene surface.

Although the surface diffusion is consistent with bulk diffusion qualitatively, quantitatively there may exist a gap between the two diffusions. For the bulk diffusion, the diffusion coefficient can be predicted from the following equation based on the hard sphere model of ideal gases,

$$D = \frac{1}{3}\bar{u}_A\lambda \quad (6)$$

where $\bar{u}_A$ is the root-mean-square velocity of molecules and λ is the mean free path of gas molecules. According to the ideal gas kinetic theory, $\bar{u}_A$ is

$$\bar{u}_A = \sqrt{\frac{8k_BTN_A}{\pi M}} \quad (7)$$

where k_B is the Boltzmann constant, T is the gas temperature, N_A is the Avogadro constant, and M is the mass of a gas molecule. The free path λ is

$$\lambda = \frac{1}{\sqrt{2}\pi d^2 N} \quad (8)$$

where d is the molecular diameter and N is the molecular number density, which can be obtained from the ideal gas state equation, as follows:

$$N = \frac{P}{k_BT} \quad (9)$$

where P is the pressure of the gas system.

Then, we compare the surface diffusion coefficients with the bulk diffusion coefficients predicted using the hard sphere model described above (see Fig. 5). Basically, the surface diffusion coefficients are lower than the bulk diffusion coefficients, especially for the CO_2 molecules with stronger adsorption ability on the graphene surface. In the adsorption layer on the graphene surface, the free motion of gas molecules is restricted not only by the neighboring molecules in the high-density zone but also by the graphene film due to the interaction between graphene atoms and gas molecules. Therefore, the surface diffusion on the graphene surface is suppressed compared to the bulk diffusion and the suppression degree of CO_2 molecules with a higher number density in the adsorption layer is higher than that of CH_4 molecules. Namely, for CO_2 molecules the surface diffusion coefficients are obviously lower than the bulk diffusion coefficients, while for CH_4 molecules the surface diffusion coefficients are slightly lower than the bulk diffusion coefficients. In short, the surface diffusion on the graphene film just follows the bulk diffusion qualitatively, and only a difference exists quantitatively due to the appearance of gas–graphene interactions.

Probability distribution of moving length

In order to further explain the reduced diffusion coefficients on the graphene surface, we obtain the probability distribution of the molecular moving length in a certain time period on the graphene surface. The moving length of gas molecules in the x–y plane occurred in a period of 250 timesteps is calculated and the probability distribution of the moving length during the MD simulation of 2 million timesteps is statistically obtained. Fig. 6 shows the moving length *versus* the corresponding occurrence number both for CH_4 and CO_2 molecules at different pressures. It is found that the probability distribution of the moving length is a regular distribution; namely, for the small and large moving lengths the probabilities are low, while for the middle moving lengths the probabilities are high. This distribution can also reflect that the gas diffusion on the graphene surface is controlled not by the hopping mechanism but by the molecular collisions, because only the gas diffusion controlled by molecular collisions can produce the regular probability distributions of the molecular moving length, where the probability of zero-moving length is exactly equal to zero and the value of the moving length is arbitrary in a certain range. With increasing the pressure, the occurrence number of a certain moving length increases, because the total number of molecular diffusion samples is larger at higher pressures. Compared to CO_2 molecules, the probability distributions of CH_4 molecules are wider and have a higher average value of moving length. This phenomenon indicates that the average velocities of CH_4 molecules on the graphene surface are higher than those of CO_2 molecules, consisting with the higher diffusion coefficients of CH_4 molecules (see Fig. 5). In addition, at a certain pressure the total occurrence number of CO_2 molecules is higher than that of CH_4 molecules, because the CO_2 molecules have stronger adsorption abilities on the graphene surface and more molecules can appear in the adsorption layer.

From the probability distribution of the moving length, we can obtain the average moving length at different pressures. As seen from the inserted data plots in Fig. 6, the average value of the moving length has a weak dependence on the gas pressure. The diffusion coefficient is related both to the velocity and the mean free path of gas molecules moving on the graphene surface, as shown in eqn (6). The independence of

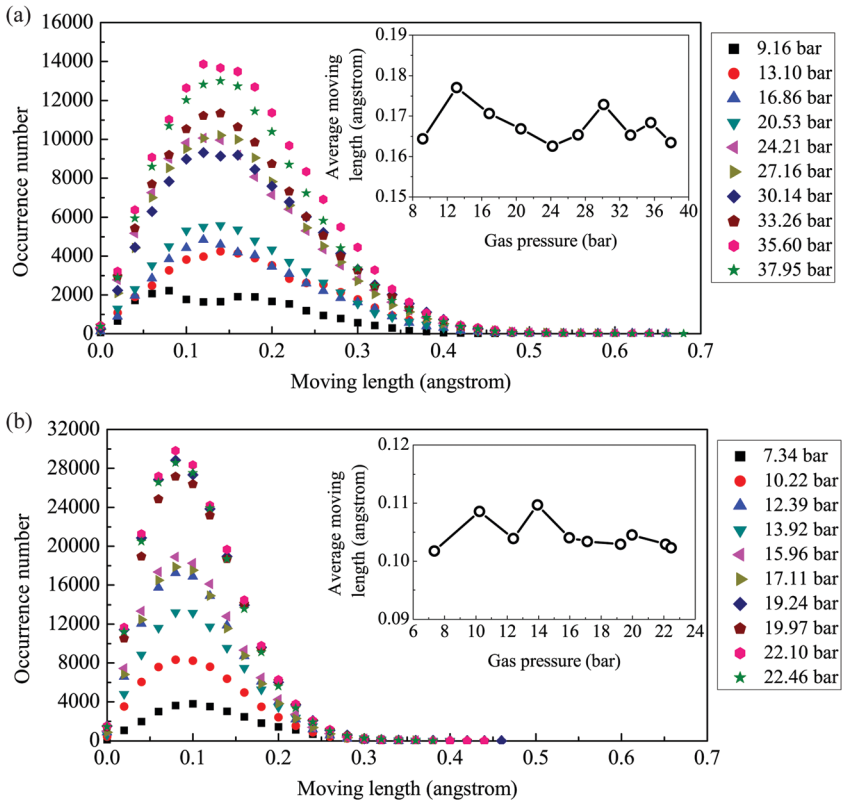

Fig. 6 Probability distribution of the moving length of gas molecules on graphene surface for (a) CH_4 and (b) CO_2, respectively. The inserted figures show the variation of average moving length *versus* gas pressure.

the average moving length on the gas pressure indicates that the molecular velocity has a weak dependence on the gas pressure. Recalling with the decrease of surface diffusion coefficient with increasing gas pressure (see Fig. 5), it can be concluded that the lower surface diffusion coefficients at higher gas pressures are mainly caused by the shortening of the mean free path of gas molecules. This conclusion is also consistent with the hard sphere model of gas diffusion (see eqn (7)–(9)), further indicating that the gas diffusion on the graphene surface is controlled not by the hopping mechanism but by the molecular collisions. Coupling the experience time of 250 timesteps, the average velocities of gas molecules moving on the graphene surface, regardless of the weak effect of pressure, are estimated to be 497.61 m s^{-1} and 317.64 m s^{-1} for CH_4 and CO_2, respectively. Compared with the root-mean-square velocity of molecules (629.97 m s^{-1} and 379.89 m s^{-1} for CH_4 and CO_2, respectively) in bulk diffusion calculated from eqn (7), the velocities of molecules on the graphene surface decrease by 21.0% and 16.4% for CH_4 and CO_2, respectively. However, the diffusion coefficients in the surface diffusion on average decrease by 44.4% and 84.3% for CH_4 and CO_2, respectively, compared to those in bulk diffusion. Hence, it can be concluded that the mean free path on the graphene surface also decreases drastically both for CH_4 and CO_2 molecules. This means that the average frequency of molecular collisions and the average travelling distance between successive collisions (mean free path) are both suppressed on the graphene surface to induce a lower diffusion coefficient.

Effect of surface functionalization

Due to the gas-like behaviors of gas diffusion on graphene surfaces, the crystal structure of the graphene surface may have a slight effect but the surface functionalization can exert an obvious influence for the presence of other chemical groups. Thus, we finally explore the effect of chemical functionalization of the graphene surface on the gas diffusion characteristics. In order to reduce the complexity of the model construction in simulations, we employ a hydrogen-functionalized graphene (HFG) to study the effect of surface functionalization. The HFG can be really realized, as demonstrated in the reported experiments.[45,46] In the HFG modeled in the simulation, 44 hydrogen atoms are uniformly functionalized on the graphene surface of area 3 × 3 nm^2. As shown in Fig. 7, there is also a monolayer of gas molecules adsorbed on the HFG surface. For convenience, the demarcation line between the adsorption layer and the gas phase is still fixed at z_m = 0.6 nm according to the number density distribution along the direction perpendicular to the surface. After the hydrogen functionalization on the graphene surface, the adsorption intensities of gas molecules on the surface are weakened, as shown in Fig. 3, which gives a comparison between the isothermal adsorption characteristics of CH_4 and CO_2 molecules on the graphene surface and that on the HFG surface. On the HFG surface, a

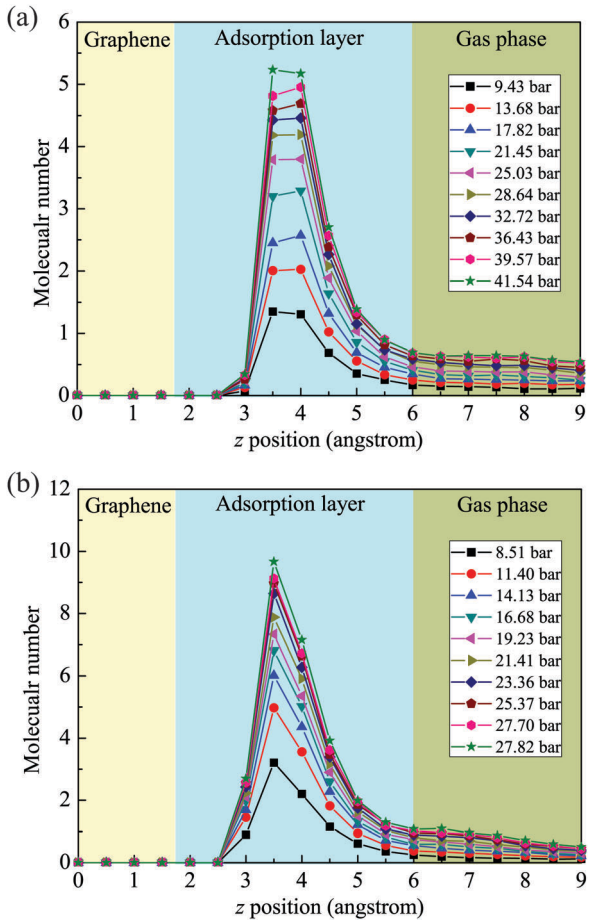

Fig. 7 Molecular number density distributions on the HFG surface for (a) CH_4 and (b) CO_2 molecules, respectively.

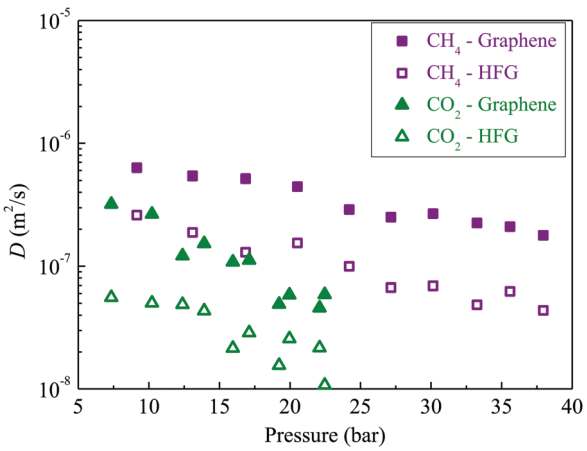

Fig. 8 Comparison between the diffusion coefficients on graphene surface and those on HFG surface.

part of the adsorption sites is occupied by the functionalized hydrogen atoms and thus the number of molecules that can be adsorbed is reduced, although the interactions between graphene and gas molecules may change slightly due to the presence of hydrogen atoms. It is noted that the gas adsorption is still purely physical adsorption without involving any chemical interactions although the chemical functional groups appear on the graphene surface.

It is generally thought that the surface diffusion coefficients on the HFG surface can be improved owing to the lower molecular density in the adsorption layer. In contrast, the surface diffusion coefficients on the HFG surface are lower than those on the graphene surface both for CH_4 and CO_2 molecules, as shown in Fig. 8. On the HFG surface, the hydrogen atoms greatly affect the surface diffusion, by blocking the motion of gas molecules on the graphene surface and shortening the free path of gas molecules. It is noted that the mechanisms identified here are also basically suitable for exploring the effects of other chemical functionalizations on the graphene surface, although these mechanisms are approved by the simplest functionalization with hydrogen atoms.

Conclusions

We study the gas diffusion on graphene surfaces using the MD simulation method, by calculating diffusion coefficients based on the Einstein equation and analyzing molecular adsorption and kinetic motion characteristics on the graphene surface. Owing to the weak gas adsorption energy, the traditional hopping model fails to describe the gas diffusion on the graphene surface for physically adsorbed gases, which is a two-dimensional gas behavior and mainly controlled by the collisions between adsorbed molecules. With increasing gas pressure, the density of adsorbed monolayer molecules increases following the Langmuir isothermal model and accordingly the diffusion coefficient decreases due to the weakened free motions of gas molecules. The restriction of the graphene film causes a reduction in the diffusion coefficient, consequently the hard sphere model for bulk diffusion overestimates the surface diffusion coefficient, especially for the CO_2 molecules with stronger adsorption ability. To be specific, the average frequency of molecular collisions and the mean free path of molecules are both suppressed on the graphene surface to induce a lower surface diffusion coefficient. In addition, the effect of surface functionalization on gas diffusion is revealed through an example of a HFG surface, which exhibits a lower diffusion coefficient of gas molecules owing to the blocking effects of chemical functional groups.

Acknowledgements

We acknowledge the financial support from the National Natural Science Foundation of China for Distinguished Young Scientists (51425603) and project No. 51506166.

References

1 C. Chmelik and J. Karger, *Chem. Soc. Rev.*, 2010, **39**, 4864–4884.
2 N. E. R. Zimmermann, B. Smit and F. J. Keil, *J. Phys. Chem. C*, 2012, **116**, 18878–18883.

3 E. A. Kotomin, Y. A. Mastrikov, E. Heifetsa and J. Maier, *Phys. Chem. Chem. Phys.*, 2008, **10**, 4644–4649.
4 E. Garcia-Perez, P. Serra-Crespo, S. Hamad, F. Kapteijn and J. Gascon, *Phys. Chem. Chem. Phys.*, 2014, **16**, 16060–16066.
5 Y. D. Chen and R. T. Yang, *AIChE J.*, 1991, **37**, 1579–1582.
6 S.-T. Hwang and K. Kammermeyer, *Can. J. Chem. Eng.*, 1966, **44**, 82–89.
7 R. T. Yang, J. B. Fenn and G. L. Haller, *AIChE J.*, 1973, **19**, 1052–1053.
8 E. R. Gilliland, R. F. Baddour, G. P. Perkinson and K. J. Sladek, *Ind. Eng. Chem. Fundam.*, 1974, **13**, 95–100.
9 A. K. Geim and K. S. Novoselov, *Nat. Mater.*, 2007, **6**, 183–191.
10 A. K. Geim, *Science*, 2009, **324**, 1530–1534.
11 K. Celebi, J. Buchheim, R. M. Wyss, A. Droudian, P. Gasser, I. Shorubalko, J.-I. Kye, C. Lee and H. G. Park, *Science*, 2014, **344**, 289–292.
12 C. Sun, B. Wen and B. Bai, *Sci. Bull.*, 2015, **60**, 1807–1823.
13 S. P. Koenig, L. D. Wang, J. Pellegrino and J. S. Bunch, *Nat. Nanotechnol.*, 2012, **7**, 728–732.
14 B. Wen, C. Sun and B. Bai, *Phys. Chem. Chem. Phys.*, 2015, **17**, 23619–23626.
15 C. Sun, B. Wen and B. Bai, *Chem. Eng. Sci.*, 2015, **138**, 616–621.
16 L. W. Drahushuk and M. S. Strano, *Langmuir*, 2012, **28**, 16671–16678.
17 C. Sun, M. S. H. Boutilier, H. Au, P. Poesio, B. Bai, R. Karnik and N. G. Hadjiconstantinou, *Langmuir*, 2014, **30**, 675–682.
18 A. Politano and G. Chiarello, *Carbon*, 2013, **62**, 263–269.
19 Y. Zhang, Q. Fu, Y. Cui, R. Mu, L. Jin and X. Bao, *Phys. Chem. Chem. Phys.*, 2013, **15**, 19042–19048.
20 L. Jin, Q. Fu, Y. Yang and X. Bao, *Surf. Sci.*, 2013, **617**, 81–86.
21 A. J. Du, Z. H. Zhu and S. C. Smith, *J. Am. Chem. Soc.*, 2010, **132**, 2876.
22 R. F. Lu, D. W. Rao, Z. L. Lu, J. C. Qian, F. Li, H. P. Wu, Y. Q. Wang, C. Y. Xiao, K. M. Deng, E. J. Kan and W. Q. Deng, *J. Phys. Chem. C*, 2012, **116**, 21291–21296.
23 M. D. Ganji, S. M. Hosseini-khah and Z. Amini-tabar, *Phys. Chem. Chem. Phys.*, 2015, **17**, 2504–2511.
24 A. Politano, M. Cattelan, D. W. Boukhvalov, D. Campi, A. Cupolillo, S. Agnoli, N. G. Apostol, P. Lacovig, S. Lizzit, D. Farías, G. Chiarello, G. Granozzi and R. Larciprete, *ACS Nano*, 2016, **10**, 4543–4549.
25 S. S. Varghese, S. Lonkar, K. K. Singh, S. Swaminathan and A. Abdala, *Sens. Actuators, B*, 2015, **218**, 160–183.
26 R. K. Paul, S. Badhulika, N. M. Saucedo and A. Mulchandani, *Anal. Chem.*, 2012, **84**, 8171–8178.
27 H. Tachikawa, *J. Phys. Chem. C*, 2008, **112**, 10193–10199.
28 X. Fan, W. T. Zheng and J.-L. Kuo, *ACS Appl. Mater. Interfaces*, 2012, **4**, 2432–2438.
29 A. M. Suarez, L. R. Radovic, E. Bar-Ziv and J. O. Sofo, *Phys. Rev. Lett.*, 2011, **106**, 146802.
30 L. R. Radovic, A. Suarez, F. Vallejos-Burgos and J. O. Sofo, *Carbon*, 2011, **49**, 4226–4238.
31 C. Uthaisar and V. Barone, *Nano Lett.*, 2010, **10**, 2838–2842.
32 C.-Z. Sun, W.-Q. Lu, B.-F. Bai and J. Liu, *Chin. Sci. Bull.*, 2014, **59**, 2478–2485.
33 H. L. Du, J. Y. Li, J. Zhang, G. Su, X. Y. Li and Y. L. Zhao, *J. Phys. Chem. C*, 2011, **115**, 23261–23266.
34 T. Wu, Q. Xue, C. Ling, M. Shan, Z. Liu, Y. Tao and X. Li, *J. Phys. Chem. C*, 2014, **118**, 7369–7376.
35 L. Li, J. Mo and Z. Li, *Phys. Rev. Lett.*, 2015, **115**, 134503.
36 S. J. Stuart, A. B. Tutein and J. A. Harrison, *J. Chem. Phys.*, 2000, **112**, 6472–6486.
37 A. M. Brockway and J. Schrier, *J. Phys. Chem. C*, 2013, **117**, 393–402.
38 A. V. Bolesta, L. Zheng, D. L. Thompson and T. D. Sewell, *Phys. Rev. B: Condens. Matter Mater. Phys.*, 2007, **76**, 224108.
39 B. Ni, S. B. Sinnott, P. T. Mikulski and J. A. Harrison, *Phys. Rev. Lett.*, 2002, **88**, 205505.
40 A. Delcorte and M. Debongnie, *J. Phys. Chem. C*, 2015, **119**, 25868–25879.
41 J. G. Harris and K. H. Yung, *J. Phys. Chem.*, 1995, **99**, 12021–12024.
42 J. Schrier, *ACS Appl. Mater. Interfaces*, 2012, **4**, 3745–3752.
43 H. Liu, S. Dai and D. Jiang, *Nanoscale*, 2013, **5**, 9984–9987.
44 H. Liu, Z. Chen, S. Dai and D.-E. Jiang, *J. Solid State Chem.*, 2015, **224**, 2–6.
45 Q. X. Pei, Y. W. Zhang and V. B. Shenoy, *Carbon*, 2010, **48**, 898–904.
46 L. Gan, J. Zhou, F. Ke, H. Gu, D. Li, Z. Hu, Q. Sun and X. Guo, *NPG Asia Mater.*, 2012, **4**, e31.

